Network performance analysis of laser-optical tracking for space situational awareness in the Lower Earth Orbit

Stefan Scharring, Jens Rodmann[1], Wolfgang Riede
German Aerospace Center (DLR), Institute of Technical Physics, Stuttgart, Germany

ABSTRACT

In our paper, recent findings from a large system study on the performance of a global laser-ranging network are presented. Whereas the simulation methodology has been presented earlier at AMOS 2018, the current work shows a detailed performance analysis with respect to representative orbital element classes, available or conceivable station sites as well as realistic observability restrictions due to cloud coverage.

For simulation configuration, orbital parameters of space objects in the Low Earth Orbit (LEO) have been statistically analyzed and clustered. A set of six orbit types with different semi-major axes and inclinations has been identified as representative for approximately 75% of all current LEO objects. For this selection, laser ranging networks of different sizes from 5 up to 50 laser ranging stations have been investigated.

Simulations of laser-based measurements from each ranging network are analyzed in terms of orbit determination accuracy and covariance propagation. Whereas the former is reviewed during a 30-day period of target tracking, the latter is considered both in-between two different station transits with laser ranging as well as for a subsequent 5-day period without any further ranging measurements. For network performance characterization, the remaining position uncertainty of laser ranging data serves as a figure of merit.

In particular, the results on network performance are mirrored against different configurations of the global station distribution under consideration of the respective orbital parameters. Moreover, network performance results are characterized with respect to downtimes due to weather restrictions. For this purpose, an 11-year month-specific statistics on the diurnal variations of cloud coverage and wind data (based on re-analysis of past weather) at each ranging location is employed.

Requirements on network sizing and station distribution are discussed with respect to operational demands in space situational awareness. In sum, a networking approach in laser ranging constitutes a viable technology for the reduction of prevailing uncertainties in orbital data of LEO objects and can particularly be expected to serve as a prerequisite for future improvement for various SSA (Space Situational Awareness) use cases, e.g. conjunction analysis, collision risk assessment, collision avoidance, re-entry events, active debris removal, and proximity operations.

1. INTRODUCTION

The expected significant increase of space launch activities in the next years and decades, both in the governmental as in the private sector, yields an enhanced risk of space debris generation. In this regard, space situational awareness is mandatory not only for the protection of active space missions, but as a prerequisite to prevent aggravation of the space debris environment by cascading effects of secondary debris generation due to in-space collisions.

High accuracy in laser ranging to space objects (within a meter or better) has already been demonstrated, e.g., by the ILRS (International Laser Ranging Service) network. Therefore, laser ranging can be considered as a highly promising sensor technology for space surveillance in the Low Earth Orbit (LEO) which has the potential to complement existing radar facilities in terms of achievable state vector accuracy.

[1] present address: etamax space GmbH, Braunschweig, Germany

However, as an optical ranging method, laser ranging requires clear skies and, at the current state-of-the-art, terminator conditions at the laser ranging site in order to allow for target acquisition and tracking. Hence, the performance of any laser ranging network is strongly affected by orbital parameters of the observation targets, laser station distribution and local weather conditions.

2. SIMULATION FRAMEWORK

The LARANEWA (Laser Ranging Network Analysis Project) simulation environment has been described in greater detail in [1] already and shall, therefore, only be summarized here, cf. Figure 1:

1. In order to allow for a realistic assessment of global laser ranging station networks, three real-world databases are employed, namely the USSTRATCOM (United States Strategic Command) catalogue for orbital elements for LEO space objects in the form of TLEs (Two-Line-Elements), a facility database compiled from publically available sources, cf. [1], and, with ERA-Interim (Reanalysis of the European Centre for Medium-Range Weather Forecasts, ECMWF), a global weather database.
2. Pre-processing is applied to each database in terms of a cluster analysis of orbital parameters, cf. sec. 3, random generation of laser station networks, cf. sec. 4, and station-specific weather data interpolation and statistics, cf. sec. 5, respectively,
3. Representative sample orbits, network station information and station weather data which altogether serve as simulation configuration and data input.
4. The main simulation is run by a Python-based script named ODSIM which comprises network setup, emphemerides and station passes calculation, weather-related pass filtering as well as the generation of artificial laser ranging measurement data and their orbital propagation for a timespan greater than one month.
5. For this purpose, various functionalities of STK (Systems Toolkit) and ODTK (Orbit Determination Toolkit) are employed by ODSIM. STK and ODTK are commercial software tools available from Analytical Graphics, Inc. (AGI) and were integrated into ODSIM using Python wrapper routines based on the STK Integration module.
6. Finally, the simulation results itself constitute a large database on laser ranging networks, accompanied by visualizations on target accessibility and measurement accuracy.

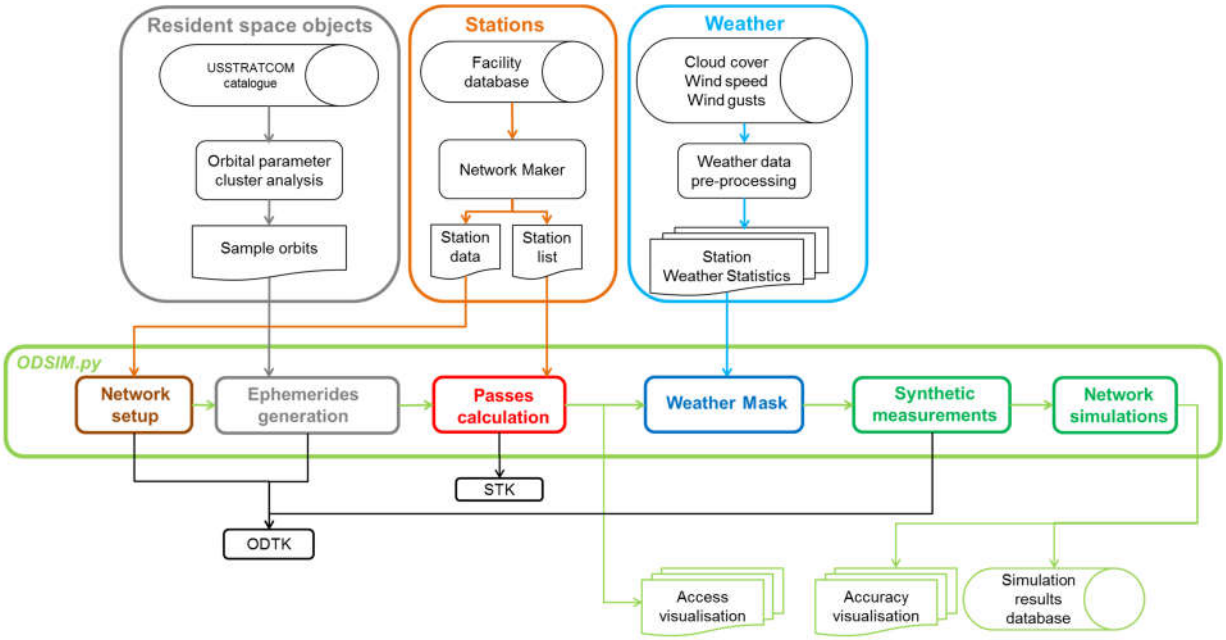

Figure 1. Flowchart of the LARANEWA simulation environment.

3. LEO ORBITS

In order to derive representative target satellites for our laser ranging simulations, a snapshot of all LEO objects in the USSTRATCOM catalogue [2] as of Nov 14, 2018, was investigated with respect to the number distributions of the respective orbital parameters.

The eccentricity of a LEO orbit is usually rather low in the range of $e \approx 0.005$ which can be ascribed to the uncertainties of circularization maneuvers. Moreover, parameters of the orbit like argument ω of perigee and mean anomaly M are nearly uniformly distributed throughout the analyzed orbital regime. The number distribution of RAAN (right ascension of the ascending node) exhibits certain maxima for $\Omega < 50°$ and $\Omega > 290°$ but also shows a large offset of orbits with uniformly distributed Ω. In contrast, we have found two of six orbital parameters being suitable for clustering, namely the semi-major axis and the inclination angle, cf. Figure 2 which shows distinct maxima. Hence, we identified six clustering centers yielding representative the LEO orbits shown in Table 1 which were analyzed in our network simulations. Doing this, approximately 75% of overall 13,714 LEO objects are represented.

For each orbit, the simulation target satellite was assumed to have a mass of 100 kg and a cross-sectional area of 1m². The initial orbit uncertainties before the first laser ranging measurement was set to 500 m (radial), 2000 m (in-track), and 1000 m (cross-track), which are typical for TLE-derived ephemerides. Ephemeris generation, orbit determination, and orbit propagation was undertaken using a 21st order geopotential and DTM 2012 as atmosphere density model.

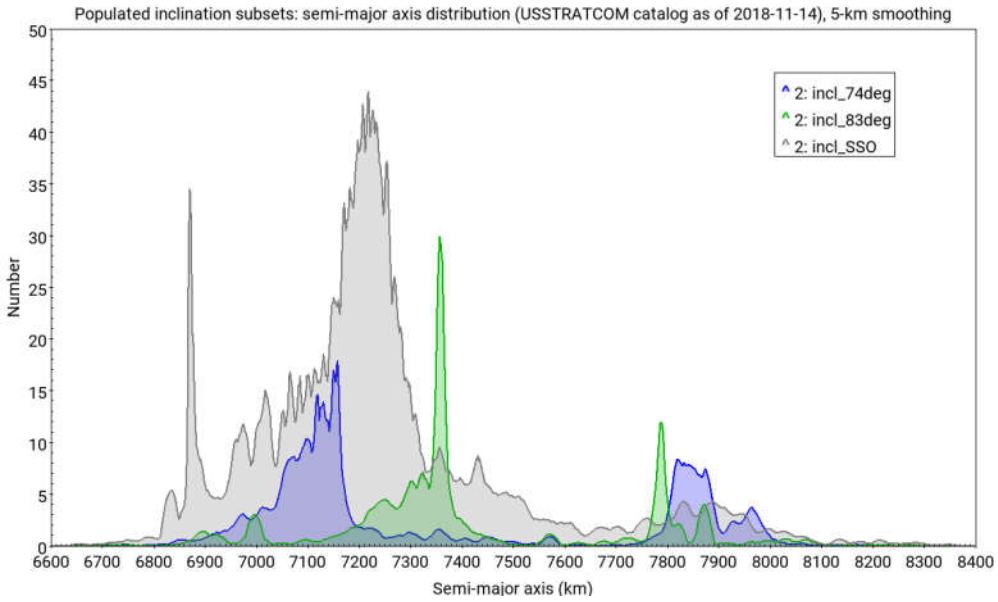

Figure 2. Semi-major axis of LEO objects: Number distribution for populations of different inclination angles (~74°, ~83°, and sun-synchronous).

Table 1. Characteristic LEO orbits for laser ranging network simulations with representative settings for the semi-major axis a and the orbit inclination angle i. Eccentricity is set $e = 0$ whereas the orbit attitude parameters Ω, ω, and M are attributed arbitrary values from a uniform distribution in $[0; 2\pi]$.

ID	Orbit type	Semi-major axis, km	Inclination	Number of objects
HI1	High inclination, low orbit	7150	74	1896
HI2	High inclination, high orbit	7850	74	
NP1	Near polar, low orbit	7355	83	1421
NP2	Near polar, high orbit	7785	83	
SSO1	Low Sun-synchronous orbit	6870	97.37	6904
SSO2	High Sun-synchronous orbit	7220	98.78	

4. NETWORK CONFIGURATION

In our simulations network sizes of $N = 5, 10, 20,$ and 46 stations, i.e., covering almost one order of magnitude, have been investigated. For their configuration N geolocations have been randomly chosen using a spherical Fibonacci lattice which provides a nearly uniform distribution of points on the sphere. For each point, the nearest laser station of our station database was selected as laser ranging network station. The global database comprises 425 sites with basic infrastructure and has been described in greater detail in our previous paper [1].

The resulting station networks are shown in Figure 3. Since all station data were collected from public resources, technical details were not similarly available throughout the database. Hence, in the sense of a first baseline study, for each station the same ranging performance was assumed. In order to simulate real measurement data, a Gauss-Markov filter was applied to the orbital data adding white noise with a bias of 1 m, a standard deviation of 0.1 m, and a half-life time of 60 min.

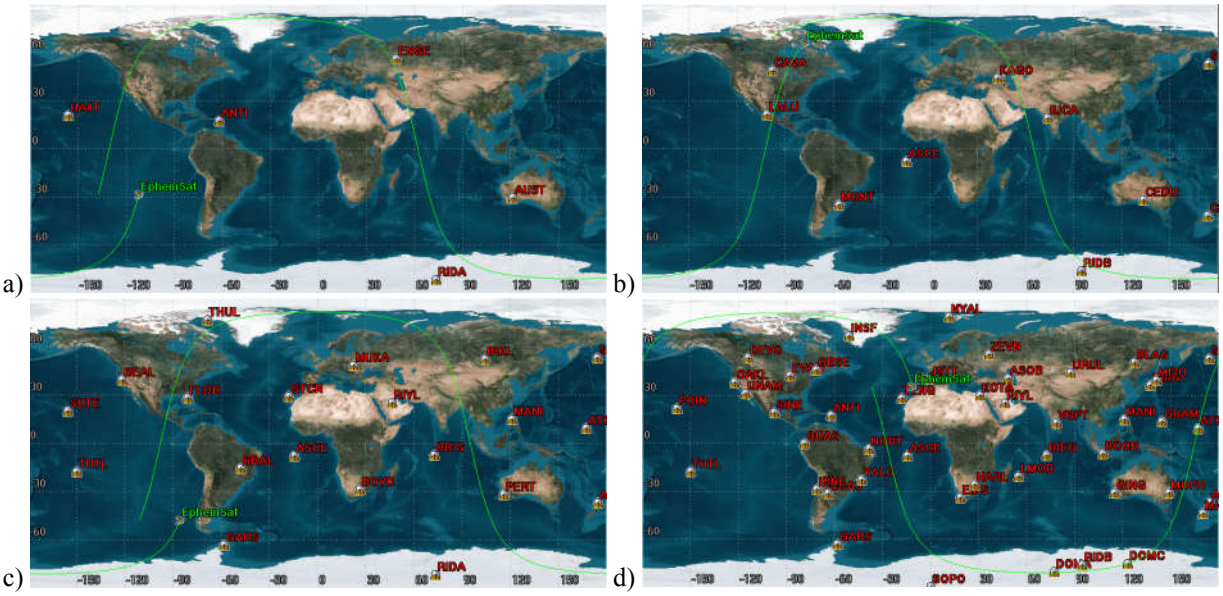

Figure 3. Simulation networks with a) $N = 5$, b) $N = 10$, c) $N = 20$, and d) $N = 46$ laser ranging sites and a sample SSO2 ground trajectory.

5. STATION WEATHER

The availability of a laser station for ranging observations is subject to various weather conditions with respect to technical feasibility of a ranging measurement as well as operational safety.

For the latter, we apply empirical constraints for safe dome operation constituting of a maximum wind speed $WS_{th} = 40\ km/h$ as well as a maximum speed of wind gusts of $WG_{th} = 65\ km/h$ [1]. Moreover, regarding the technical feasibility of laser ranging measurements it is mandatory that the line of sight from the laser station to the space object is free of clouds. This does not necessarily require an entirely clear sky, but the respective cloud fraction should not exceed a certain limit. Therefore, we analyzed laser observation timeslots at our ILRS Engineering Station Stuttgart Uhlandshöhe (IRLS code UROL) with respect to cloud fraction data from the recent years, cf. Figure 4. It can be seen that a significant increase in the number of observations is found with a cloud cover fraction of $CF \leq 0.25$ whereas for $CF \geq 0.5$ observation outages due to cloud cover are more likely. Hence, in our simulations we have chosen $CF_{th} = 0.5$ as a threshold value to determine whether a laser ranging measurement is feasible or not.

In order to assess the weather conditions at the particular sites, global data on CF, WS, and WG have been obtained from various databases of the European Center for Medium Weather Forecast (ECMWF) [6] Those data constitute a re-analysis of weather data from various sources (satellite observations, ground-based and air-borne measurements)

against numerical weather prediction models. They are available on a grid with 0.75° resolution (latitude, longitude) with a 3-hourly temporal resolution. Thus, we are able to derive station weather data using grid interpolation for each of the 425 laser ranging sites on a 3-hour base covering the years from 2007 to 2017.

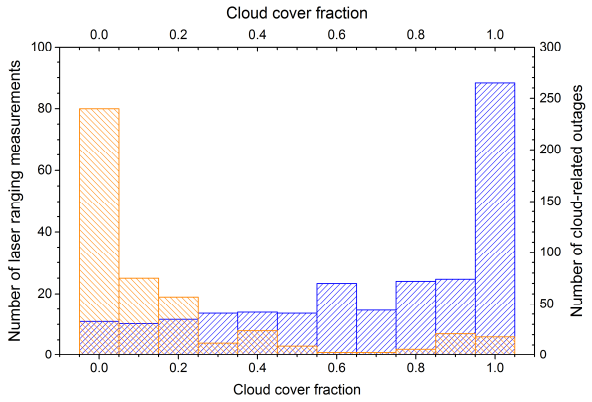

Figure 4. Interrelation of cloud coverage and observation times at the laser ranging facility Stuttgart-Uhlandshöhe, Germany, from April 2013 to June 2016.

It has to be noted here, that due to, e.g., the specific topography of a given laser site, the local microclimate might significantly differ from the interpolated values of the ECMWF data. Nevertheless, the data appear to be suitable for a first assessment of weather conditions in laser ranging due to their sound observational database in connection with the long-term heritage of validated numerical models. Moreover, note that whereas for our study ERA-Interim data have been used, a new dataset named ERA5 has been issued by the ECMWF which exhibits a superior resolution (0.3° lat/lon and 1-hourly resolution) and is available upon registration as well [7].

In addition to the used 3-hourly weather data, pre-processing has been carried out in order to derive various weather data statistics. For the scope of this study, the monthly average of each data product has been calculated for each time of the day (0000, 0300, 0600 … hours UTC). Subsequently, the resulting average and corresponding standard deviation have been averaged over all respective datasets for the years 2007 – 2017, yielding, e.g., the typical cloud fraction cover at a Maui (ILRS code HA4T) laser ranging station at 1800 UTC on a September day during 2007 – 2017, which, in this case, is $CF_{amah}(HA4T) = 0.27 \pm 0.20$ where amah is the data classifier indicating values being month-specific (m) and time-specific (h) whereas averaging (a) has been carried out over the respective years (y→a) of data coverage and days (d→a) of the corresponding month.

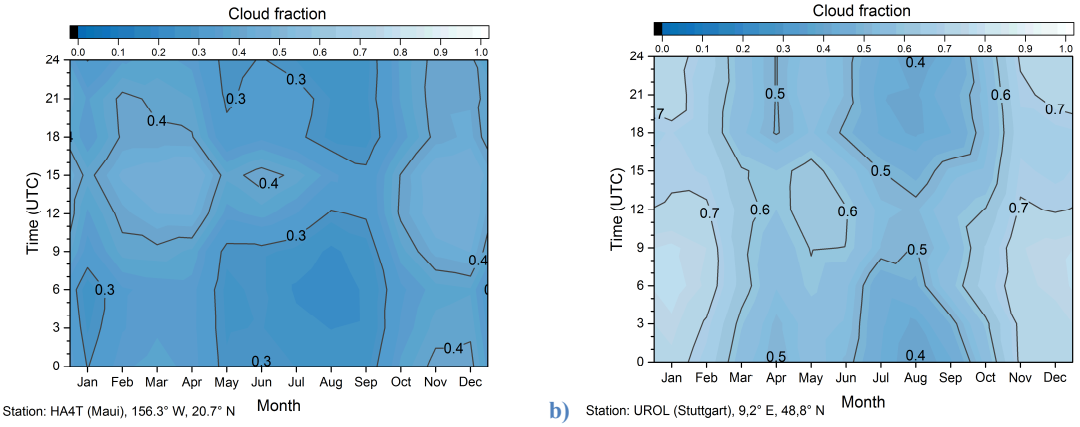

Figure 5. Average cloud cover fraction at a) Maui and b) Stuttgart, interpolated from ECMWF re-analysis data and averaged from 2007 – 2017.

In order to decide whether a specific station transit can be accessed by laser ranging or not, a random number from the Gaussian $(\langle CF \rangle, \sigma_{CF})$-distribution of the station is calculated and compared with the predefined threshold.

Accordingly, in the given example of Maui station, observability on a September's day around 1800 UTC is likely, $\langle CF \rangle + \sigma_{CF} < CF_{th}$, but not guaranteed, whereas the respective probability at Stuttgart, Germany, is much less, $CF_{amah}(UROL) = 0.44 \pm 0.37$.

Using corresponding datasets and thresholds for cloud cover, wind speed, and wind gusts, for every simulation run the list of station transits is revised deleting all transits in which one or more weather conditions prevent laser ranging observations.

6. NETWORK SIMULATIONS

$6 \times 4 \times 12 = 288$ simulation runs have been carried out taking into account for 6 different orbit types, 4 different network sizes with randomly distributed stations, and weather conditions during all 12 months of the year.

In order to account for the lower atmospheric transmissivity at low elevation angles above the local horizon as well as for laser safety concerns, a minimum elevation of 30 degrees has been assumed. To facilitate target acquisition and tracking, we set the constraint that the sun elevation shall not exceed -6 degrees whereas the space object is illuminated by the sun. Station passes meeting these requirements are registered as possible observation timeslots then in case their duration amounts at least 1 minute.

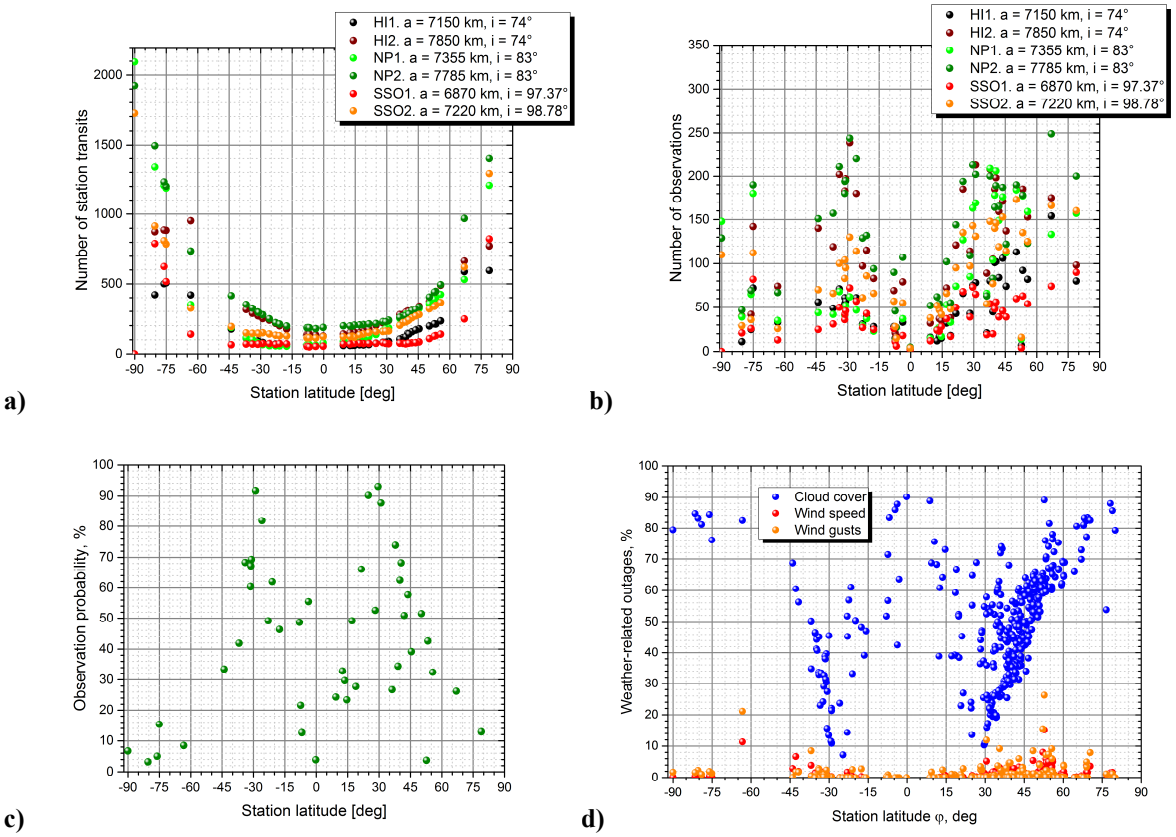

Figure 6. Visibility analysis of a simulation network with 46 laser ranging stations: a) Number of station transits in 2018 for target satellites in six different types of orbit, cf. section 3, b) number of their feasible observations under statistically representative weather conditions, c) observation probability for the given transits with respect to the weather constraints as laid out in section 5. A general analysis on weather-related downtimes for all 425 LARANEWA sites is shown in Fig. d) for the entire time range of 2007 – 2017.

As an example, the number of station transits in the largest ranging simulation network ($N = 46$) is shown in Figure 6a). Each laser station is represented there by data points at the respective station latitude given by the x-axis coordinate. It can be seen that, in general, stations at higher latitudes offer significant more accessibility for laser

ranging whereas station transits are less frequent for lower latitudes. This can be ascribed not only to the visibility of the satellite from a particular site but also to the twilight condition for the measurements restricting observational time for lower station latitudes.

On the other hand, weather conditions are generally less favorable for stations at high geographical latitude, cf. Figure 6c) which summarizes the results of the above-mentioned weather filter routine applied at the station transits in our simulations with the named network. It can be seen that, roughly speaking, that at (absolute) geographical latitudes between $|\varphi| = 15°$ and $|\varphi| = 45°$ advantageous weather conditions exist where a laser ranging measurement is rather likely than unlikely whereas at other locations the opposite is the case. Sites near the tropical circles appear to be particularly favorable whereas weather conditions are usually very unfortunate near the equator and beyond the polar circles.

In this regard, the number of transits and the weather-related observation probability show a reciprocal-like behavior to each other so that the respective benefits of a station location at low or high latitude cancel out up to a certain amount, as can be seen in Figure 6b). The equatorial region, however, constitutes an exception here, being exceptional unfortunate with respect to both weather and station passes.

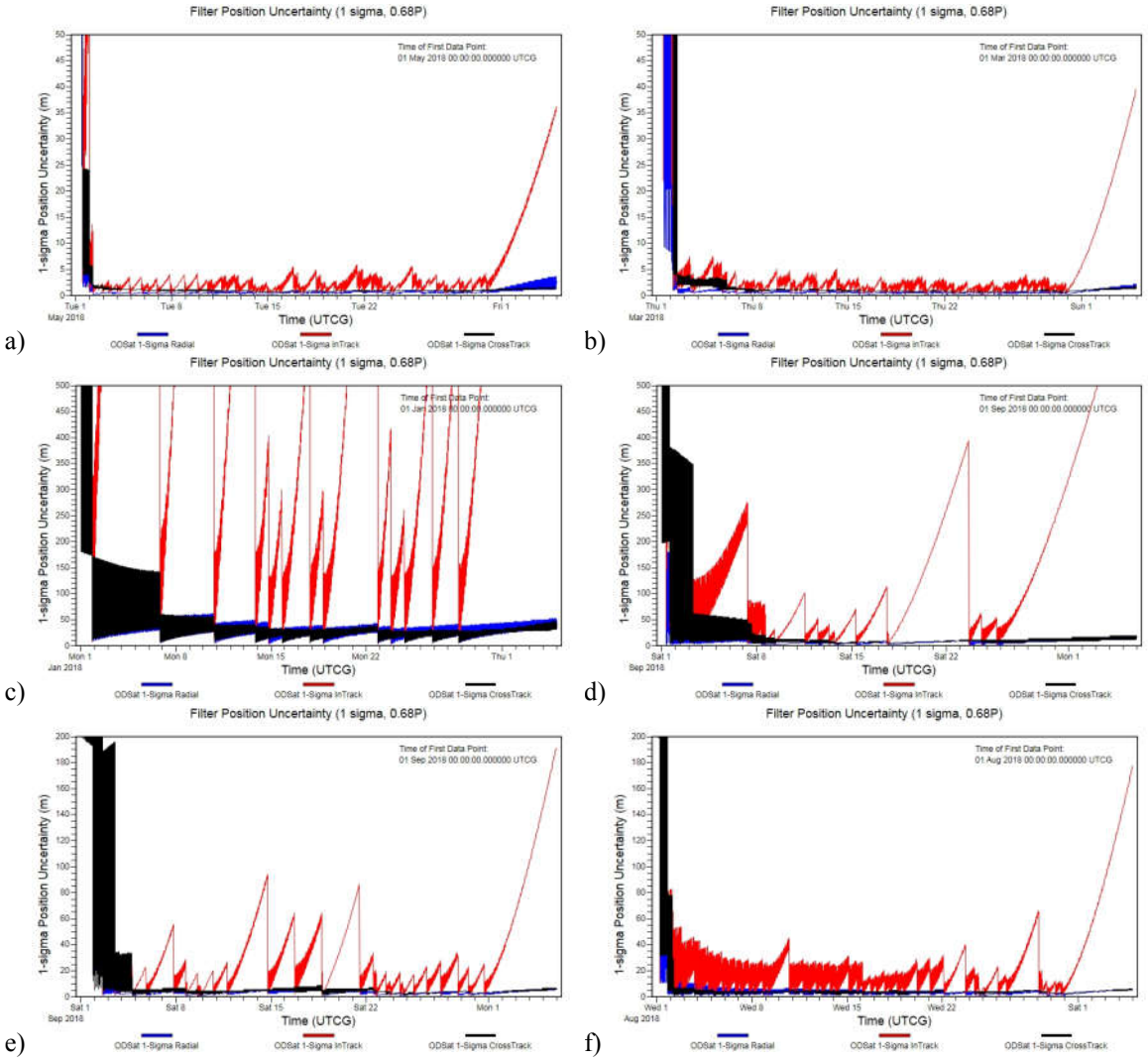

Figure 7. 1-σ position uncertainty during laser ranging measurements by a 5-station (a), c), e)) and a 10-station network (b), d), f)), respectively. Settings: a) Orbit HI2, May, b) NP 2, February, c) SSO1, January, d) SSO2, September, e) NP1, September, and f) NP1, August.

A detailed analysis on weather restrictions with respect to all stations and the whole timespan covered by our weather data is shown in Figure 6d). These restrictions greatly affect the quantity of laser-ranging measurement data during a longer period. In the case of good weather conditions, highly precise data can be obtained over a large timespan even with a small network, cf. Figure 7a) – b). Under unfavorable weather conditions, however, large measurement gaps yield correspondingly great increases of data inaccuracy which are not compliant with requirements for orbital traffic management, cf. Figure 7c) – d). For comparison, the requirement of 1-σ RIC position error of $40\ m \times 200\ m \times 100\ m$ (radial, in-track, cross-track) for at least 48 hours [8] cannot be met in the above-mentioned simulations whereas under moderate weather conditions this can already be achieved, cf. Figure 7e) – f).

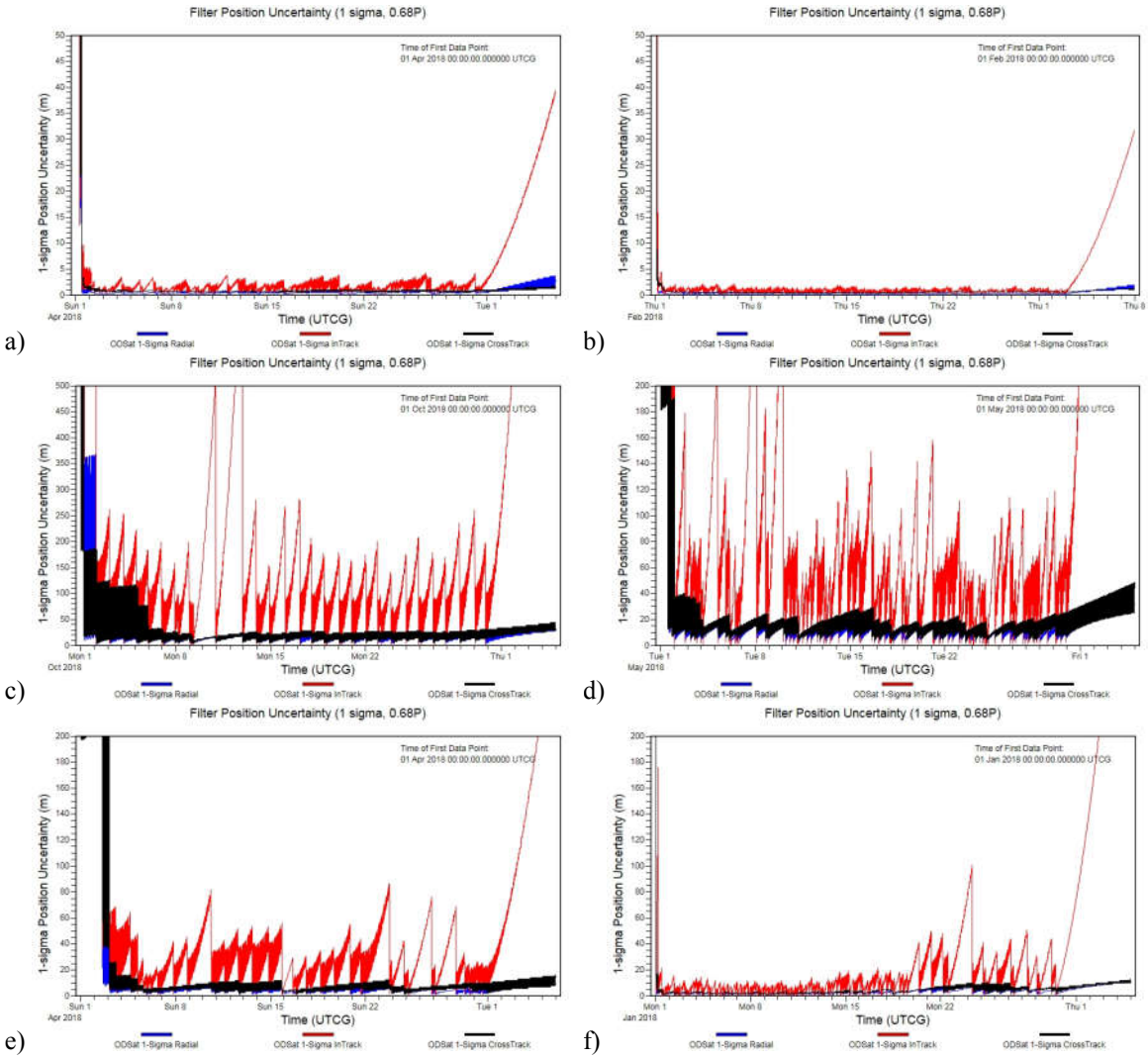

Figure 8. 1-σ position uncertainty during laser ranging measurements by a 20-station (a), c), e)) and a 46-station network (b), d), f)), respectively. Settings: a) Orbit HI2, April, b) HI2, February, c) SSO1, October, d) SSO1, May, e) SSO2, April, and f) HI1, January.

Note that the main issue here is given by the in-track uncertainty. It can be seen from the last 5 days of the temporal courses shown in Figure 7 where intentionally no measurement is undertaken that the respective uncertainty almost linearly increases in the way it does during the preceding 30 days in-between the ranging measurements, in particular pronounced during the weather-related outages. This increase of uncertainty, however, is strongly dependent on the orbit type and ranges from less than one day (SSO1), over a few days (SSO2, HI1, NP1) up to a

few weeks (NP2, HI2). This underlines the necessity of clustering orbit types for this kind of network analysis and demands for a thorough distinction of the operational orbital regime when assessing laser ranging technology.

With respect to the examples shown in Figure 8 it can be stated that even under bad weather conditions it is feasible to provide high-accuracy laser ranging data with respect to the named ESA requirements using a network of 20 stations. Only in the case of orbits where the accuracy of measured data rapidly decreases after a ranging measurement, i.e., SSO1, larger ranging networks are advisable, cf. Figure 8 c)-d).

7. SUMMARY AND OUTLOOK

A simulation framework to model the performance of networks of laser-ranging stations for SSA applications has been developed comprising sites from a global database and station-specific weather statistics. Randomly distributed networks have been setup for size from 5 to 46 sites for the simulation of synthetic laser-ranging measurements of orbital assets residing on six different representative LEO orbit types identified in a cluster analysis. The resulting measurement data accuracy has been analyzed during a 30-day measurement period under various seasonal weather conditions. Moreover, the long-term "orbit" quality after such a measurement campaign was assessed.

It has been shown that laser ranging measurements yield a significant improvement accuracy of orbital data. The analysis of orbit propagation after a single measurement shows, however, that the lifetime of data accuracy strongly depends of the orbit type which in turn determines the needed frequency of accuracy updates by ranging measurements. Therefore, redundancy is needed in terms of number and distribution of laser sites in order to compensate for outages due to weather restrictions. Moreover, a global station distribution is needed to cover all conceivable LEO orbits, in particular with respect to the distribution of RAAN.

The geographical distribution of laser sites should take into account for both favorable weather conditions, in particular concerning the regions around the tropic circles, as well as large numbers of overpasses, given at locations beyond the arctic circles.

In general, it can be stated that a network size of about 20 stations appears to be sufficient to keep in-track position uncertainty below approximately $500\ m$ using laser ranging measurements. In turn, radial and cross-track position uncertainty stay below $\sim 50\ m$ then.

Future work should take into account for site-specific weather conditions in greater detail. Not feasible on a global scale, location-specific weather station data from the selected laser sites should be used. Moreover, the atmospheric transmissivity should be considered in terms of aerosol optical depth as well.

Whereas the given simulation configuration is based on twilight conditions in order to facilitate target acquisition and tracking, advanced laser ranging networks should aim for 24/7 tracking which requires, after a single initial orbit determination, handover of laser ranging data between different stations for "blind" target acquisition and tracking under daylight and night conditions. This implies a trade-off between the capability to keep a large catalogue of many objects with high precision laser-based orbital data and correspondingly higher requirements for observation time coverage and station redundancy due to the restricted lifetime of data accuracy.

In particular with respect to space debris, the implementation of a laser-matter interaction module is planned in order to assess the modification of debris trajectories by ground-based high power laser using photon pressure or laser ablation with the aim of avoiding debris-debris collisions and eventually debris removal.

8. ACKNOWLEDGMENTS

This work was performed in the context of the study *Laser Ranging Network Analysis (LARANEWA)* (Study FÜ 10F H 014 X) commissioned by the Office for Defence Planning of the German Armed Forces (Planungsamt der Bundeswehr). The authors wish to thank Anja Jenner and Tim Clausen (both aerospace engineering students at the University of Stuttgart, Institute of Space Systems) for their help in compiling station data from publicly available

sources as well as developing the Network Maker GUI (Graphical User Interface). Initial training and continuous support for the software tools ODTK and STK is kindly acknowledged; Giuseppe Corrao (AGI) has been particularly helpful. We also wish to express great thanks to our colleague Daniel Hampf providing us with long-term statistics and laser-ranging observations at the Stuttgart Uhlandshöhe observatory UFO. Moreover, the access to weather data from the ECMWF is greatly acknowledged.

9. REFERENCES

[1] Rodmann, J., Riede, W., and Scharring, S., Performance of a global network of laser-optical tracking stations for LEO space surveillance, *AMOS Paper* (2018).
[2] USSTRATCOM catalogue, https://www.space-track.org.
[3] Fiedler, H., SMARTnet™ wind speed cutoff, private communication, Oct 13, 2017.
[4] McClatchey, R. A. et al., Optical Properties of the Atmosphere (3rd ed.), *Environmental Research Papers* **411**, Air Force Cambridge Research Laboratories (1972)
[5] Dee, D., The ERA-Interim reanalysis: configuration and performance of the data assimilation system, *Quarterly Journal of the Royal Meteorological Society* **137**: 553 – 597 (2011)
[6] ECMWF, ERA-Interim Re-Analysis. Daily, http://apps.ecmwf.int/datasets/data/interim-full-daily/levtype=sfc/ (last accessed May 9, 2018)
[7] ECMWF, Copernicus Knowledge Base, https://confluence.ecmwf.int/display/CKB/How+to+download+ERA5 (last accessed May 22, 2019)
[8] Krag, H., Flohrer, T., and Bobrinsky, N., ESA's SST activities and plans for the years 2017-2020, *Defense Satellites*, Conference Presentation (2016)
[9] Scharring, S., Eisert, L., Lorbeer, R.-A., and Eckel, H.-A., Momentum predictability and heat accumulation in laser-based space debris removal, *Optical Engineering* 58(1): 011004 (2018).

10. ABBREVIATIONS

CF	Cloud fraction
ECMWF	European Centre for Medium-Range Weather Forecasts
ERA-Interim	ECMWF Reanalysis
EU	European Union
GUI	Graphical User Interface
HI	High inclination
ILRS	International Laser Ranging Service
LARANEWA	Laser Ranging Network Analysis Project
LEO	Low Earth Orbit
MACC	Monitoring Atmospheric Composition and Climate
NATO	North Atlantic Treaty Organization
NP	Near polar
RAAN	Right ascension of the ascending node
ODSIM	Orbit Determination Simulation code for Laser-Ranging Measurement Networks
ODTK	Orbit Determination Tool Kit
SSA	Space Situational Awareness
SSO	Sun-synchronous orbit
STK	Systems Tool Kit
TLE	Two-Line-Element
USSTRATCOM	United States Strategic Command
WG	Wind gusts
WS	Wind speed